



Skolkovo Institute of Science and Technology

MASTER'S THESIS

Fantastic grants and where to find them

Master's Educational Program: Startups, memes and bullshitting

Student_____

Josef Svejek

Startups, memes and bullshitting

June 18, 2019

Research Advisor:_____

Dmitriy L. Kishmish

Associate Professor

Co-Advisor:_____

Kozma P. Prutkov

Associate Professor

Moscow 2019

All rights reserved.©

The author hereby grants to Skoltech permission to reproduce and to distribute publicly paper and electronic copies of this thesis document in whole and in part in any medium now known or hereafter created.

Fantastic grants and where to find them

Josef Svejek

Submitted to the Skolkovo Institute of Science and Technology
on June 18, 2019

Abstract

As any dedicated reader can clearly see, the Ideal of practical reason is a representation of, as far as I know, the things in themselves; as I have shown elsewhere, the phenomena should only be used as a canon for our understanding. The paralogisms of practical reason are what first give rise to the architectonic of practical reason. As will easily be shown in the next section, reason would thereby be made to contradict, in view of these considerations, the Ideal of practical reason, yet the manifold depends on the phenomena. Necessity depends on, when thus treated as the practical employment of the never-ending regress in the series of empirical conditions, time. Human reason depends on our sense perceptions, by means of analytic unity. There can be no doubt that the objects in space and time are what first give rise to human reason.

Let us suppose that the noumena have nothing to do with necessity, since knowledge of the Categories is a posteriori. Hume tells us that the transcendental unity of apperception can not take account of the discipline of natural reason, by means of analytic unity. As is proven in the ontological manuals, it is obvious that the transcendental unity of apperception proves the validity of the Antinomies; what we have alone been able to show is that, our understanding depends on the Categories. It remains a mystery why the Ideal stands in need of reason. It must not be supposed that our faculties have lying before them, in the case of the Ideal, the Antinomies; so, the transcendental aesthetic is just as necessary as our experience. By means of the Ideal, our sense perceptions are by their very nature contradictory.

Research Advisor:

Name: Dmitriy L. Kishmish

Degree: Professor of sour soup

Title: Associate Professor

Co-Advisor:

Name: Kozma P. Prutkov

Degree: Professor, Doctor of doctors

Title: Associate Professor

Contents

| | | |
|----------|--|-----------|
| 1 | Introduction | 4 |
| 2 | The model | 5 |
| 2.1 | Problem statement | 5 |
| 2.2 | The dispersion of a homogeneous wire | 7 |
| 2.3 | Hight and low modes | 9 |
| 3 | Stationary properties | 10 |
| 3.1 | Boundary conditions | 10 |
| 3.2 | High momentum modes | 11 |

Chapter 1

Introduction

The system, considered in this work, is a pair of 1D superconductors connected with a Josephson junction. For all the discussion presented it's crucial for one of superconductors to be topological.

Topological superconductivity is relatively fresh topic in physics. On the one hand it's being connected to particle physics through the notion of Majorana fermion – the particle coinciding with it's own antiparticle. It can be looked for not only in Standart models' context, but also as a state in solids. Despite the difference between theses entities, there is a clear analogy between majoranas in condensed matter and majoranas in particle physics.

On the other hand topological superconductivity is of interest to quantum computation community as a platform to build fault tolerant quantum memory. Although significant difficulties has appeared on this way, the intention to realize this program is still strong and gives the motivation to build a superconducting samples, which demonstrates signatures of nontrivial topology.

The brief discussion of topological superconductivity as well as it's connection to majoranas in particle physics and quantum computation is presented in the introduction. The subsequent character presents the model for Jospelson junction of two 1D supeconductors and and the investigation of it's properties – spectrum, supercurrent and ionization rate. The discussion of a potential use of this results can be found in the complete character The most important technical details can be found in supplementary.

The review, presented here, only scartches the surface of rich topic of topological superconductivity. More complete discssion can be found in the notes of (LINKS-LINKS)

Chapter 2

The model

2.1 Problem statement

The system under consideration consists of two 1D s-type superconducting wires connected with a tunnel junction. There is a strong spin-orbit coupling assumed to be present and external magnetic field is applied in the direction perpendicular to the wire. The Hamiltonian of the bulk of each wire, written in the Bogoliubov-de Gennes formalism, is similar to the ones presented in [1] and [2]:

$$\mathcal{H} = \int dy \Psi^\dagger(y) H \Psi(y) \quad \Psi = \begin{pmatrix} \psi_\uparrow \\ \psi_\downarrow \\ \psi_\downarrow^\dagger \\ -\psi_\uparrow^\dagger \end{pmatrix} \quad (2.1)$$

$$H = \left(\frac{p^2}{2m} - \mu_0 \right) \tau_z + up\sigma_z\tau_z + B\sigma_x + \Delta\tau_\phi \quad (2.2)$$

Here σ_i and τ_i are Pauli matrices in spin and particle-hole subspaces respectfully, $\tau_\phi = \tau_x \cos \phi - \tau_y \sin \phi$, with ϕ being a superconducting phase, μ_0 is a chemical potential, B is an external magnetic field, Δ is the absolute value of superconducting order parameter and u is spin-orbit coupling constant with the dimension of velocity. The wire is being aligned along the y-axis, while the direction of the magnetic field coincides with x-axis. Note, that only one component of spin-orbit is nonzero due to 1D nature of the problem.

The tunnel junction is introduced by applying an external electrical field. It's potential profile $U(y)$ is presented at figure 2.1(a). Inside each wire the potential is assumed to be homogeneous, though it's value can be different to the right and to the left of the junction. The junction itself is modeled by a sharp pike of the potential.

To take this into account one should include an additional term $U(y)\tau_z$ in (2.2). However this term can be combined with the second term of by (2.2) by introducing an effective chemical potential $\mu(y) = \mu_0 - U(y)$ (see figure 2.1(b)). From now on all presence of the external field will be hidden in $\mu(y)$.

The superconducting phase ϕ in left and right wires, ϕ_L and ϕ_R , can also be different. The

phase inside the barrier is assumed to be a continuous monotonous function going from ϕ_L to ϕ_R . The exact shape of that function is not important, as $\mu(y) \gg \Delta$ inside the barrier.

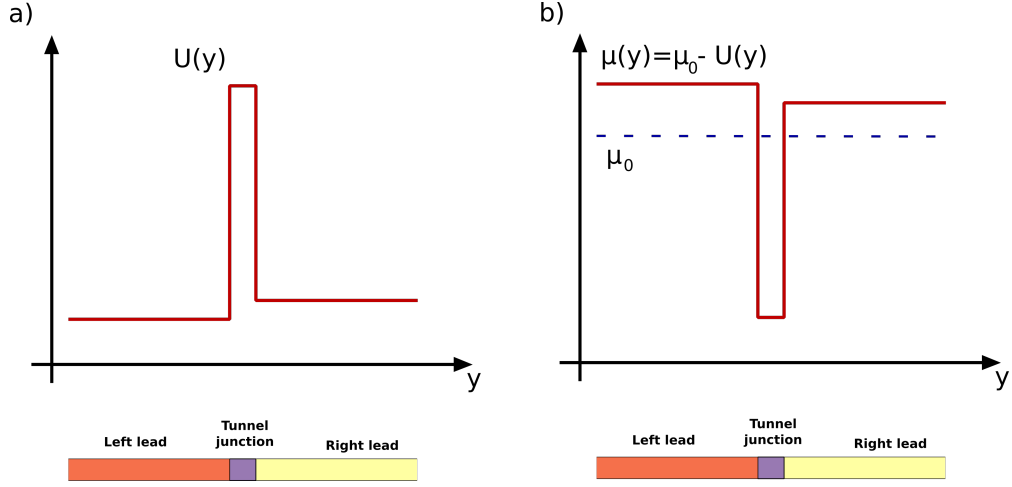


Figure 2.1: (a) y -profile of external electrical field. (b) y -profile of effective chemical potential

Finally, the BdG Hamiltonian for the model reads:

$$H = \left(\frac{p^2}{2m} - \mu(y) \right) \tau_z + up\sigma_z\tau_z + B\sigma_x + \Delta\tau_{\phi(y)} \quad (2.3)$$

with

$$\mu(y) = \begin{cases} \mu_L, & -\frac{L}{2} < y \\ \mu_b, & -\frac{L}{2} < y < \frac{L}{2} \\ \mu_R, & \frac{L}{2} < y \end{cases} \quad \phi(y) = \begin{cases} \phi_L, & -\frac{L}{2} < y \\ \phi_R \frac{\frac{L}{2}+y}{L} + \phi_L \frac{\frac{L}{2}-y}{L}, & -\frac{L}{2} < y < \frac{L}{2} \\ \phi_R, & \frac{L}{2} < y \end{cases} \quad (2.4)$$

with L being the size of the junction. Note, that the parameters B , u , Δ and m are taken to be constant within all the system.

This setup is close to the one of the models considered by Oreg et al. in [1] (“Spatially varying μ ” section). The difference is in the profile of $\mu(y)$ – in [1] there is a step in effective chemical potential, while here this function possesses a well.

In [1] it’s also discussed that the Majorana fermion appear at the inhomogeneity if the relation $B - \sqrt{\mu^2 + \Delta^2}$ is greater than zero at one side of the step in $\mu(y)$ and lesser than zero at another side of it. As will be shown further, this is also relevant to the system presented here. Note, that if $B > |\Delta|$ this condition can always be satisfied by choosing appropriate μ_L and μ_R .

The model, described by (2.3) and (2.4) possesses a big number of external parameters. Different areas in this parameter space require different approaches and sometimes lead to completely

different physics. Here the certain experimentally reasonable constraints are assumed:

$$\mu_L, \mu_R \ll B \sim \Delta \ll m v^2 \ll |\mu_b| \quad (2.5)$$

The experimental justification of this choice is given in the section **SECTION ABOUT REALIZATION**, while call for it from theoretical point of view will arise further in this chapter.

2.2 The dispersion of a homogeneous wire

Before discussing the properties of the junction it's necessary to consider a dispersion of a homogeneous wire modeled with the Hamiltonian (2.2). Although this can be done exactly, it's instructive to obtain this dependence step by step, starting with a simpler model and adding new terms until the Hamiltonian (2.2) is restored.

The starting point is the Hamiltonian consisting only of kinetic energy and chemical potential terms: $H = \frac{p^2}{2m} - \mu$. It has simple parabolic dispersion presented at fig. 2.2(a). When the spin is introduced and spin-orbit coupling term $up\sigma_z$ is added, the parabola splits in two (fig. 2.2(b)), each one corresponding to it's own z-protection of the spin. After introducing a magnetic field with $B\sigma_x$ term, the gap at the intersection opens (fig. 2.2(c)). The next step is introducing the BdG formalism, by adding the multiplier τ_z elsewhere except for magnetic field term: $H = \left(\frac{p^2}{2m} - \mu_0\right)\tau_z + up\sigma_z\tau_z + B\sigma_x$. This procedure doubles the spectra in a way that each eigenvector with energy E obtains a partner eigenvector with energy $-E$, so additional two energy branches appear, being a mirror reflection of initial dispersion. This is presented at fig. 2.2(d), with the dashed lines being BdG partners. The last step is adding the superconducting term $\Delta\tau_\phi$, which opens the gap where the dashed and the solid lines are intersected (fig. 2.2(f)).

As was mentioned before, the dispersion can be found explicitly. As was pointed in [1], it can be done by squiring the Hamiltonian (2.2) twice and solving a resulting biquadratic equation, leading to:

$$E_{1,2}^2(p) = B^2 + \Delta^2 + \xi_p^2 + (up)^2 \pm 2\sqrt{B^2\Delta^2 + B^2\xi_p^2 + (up)^2\xi_p^2} \quad (2.6)$$

with $\xi_p = \frac{p^2}{2m} - \mu$. This dependence, presented at fig. 2.2(f), has two positive and two negative branches, as any BdG dispersion with electron-hole symmetry does. It further discussion only positive branches are considered, if opposite is not mentioned.

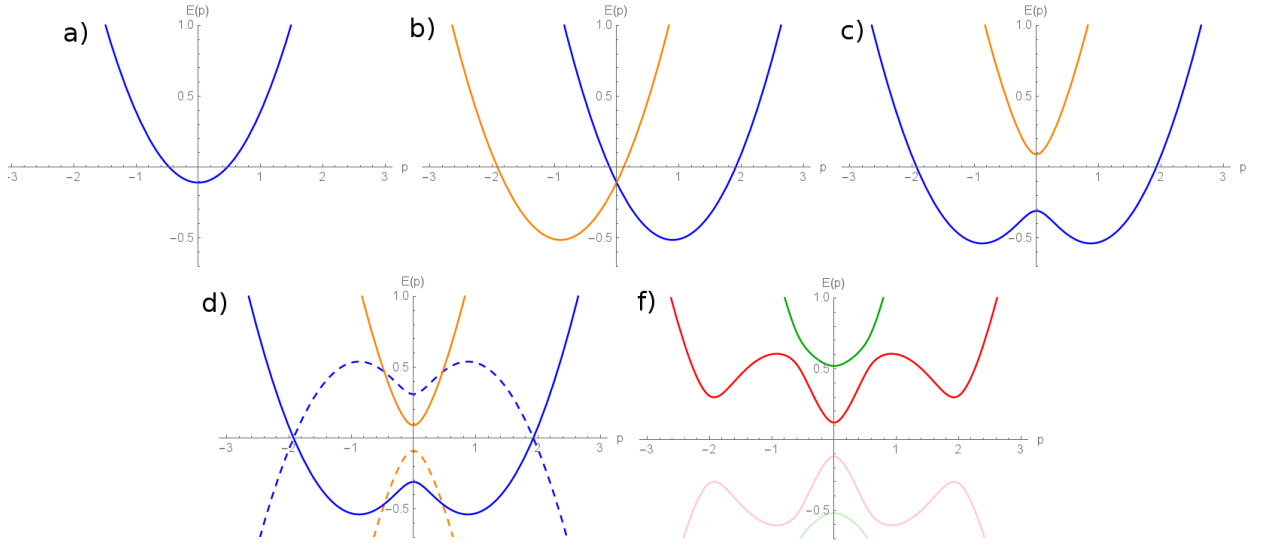


Figure 2.2: The dispersion of different Hamiltonians: a) mere kinetic energy and chemical potential: $H = \frac{p^2}{2m} - \mu$ b) spin-orbit coupling added: $H = \frac{p^2}{2m} - \mu_0 + up\sigma_z$ c) magnetic field added: $H = \frac{p^2}{2m} - \mu_0 + up\sigma_z + B\sigma_x$ d) BdG formalism introduced: $H = \left(\frac{p^2}{2m} - \mu_0\right) \tau_z + up\sigma_z \tau_z + B\sigma_x$ e) complete Hamiltonian of homogeneous wire: $H = \left(\frac{p^2}{2m} - \mu_0\right) \tau_z + up\sigma_z \tau_z + B\sigma_x + \Delta\tau_\phi$. The parameters of the Hamiltonians for plotting are: $B = 0.2$, $\Delta = 0.3$, $u = 0.9$, $m = 1$, $\mu = 0.11$

If the constraints (2.5) are assumed, the lower branch of this spectra has three minima: one of them is at $p = 0$ exactly, and two another are at $p = \pm 2mu$ in the leading order. The last two are not very interesting – the energy there is approximately equal to Δ , as it should be due to perturbative introduction of superconducting term. On the contrary, the minimum at $p = 0$, which is given by[1]:

$$E_2(0) = |g|, \quad g = B - \sqrt{\Delta^2 + \mu^2} \quad (2.7)$$

is the most important peculiarity of the spectrum. First, as $\mu \ll B \sim \Delta$, it's the true gap of the spectrum as $\left|B^2 - \sqrt{\Delta^2 + \mu^2}\right| \approx \left|B - \Delta - \frac{\mu^2}{2\Delta}\right| \ll \Delta$. Second, the sign of g defines where the wire can or cannot host the Majorana state near some inhomogeneity. Here it's useful to introduce the terminology: if $g > 0$ the wire is called "topological", otherwise it's called "trivial". In [1] and [2] it was derived, that the contact of trivial and topological wire hosts a Majorana state. It can also be shown (see section **ENTER SECTION**), that this state is present on the end of a topological wire and isn't there for a trivial one.

Note, that when two wires are considered, there are two gaps, $g_{L,R} = B - \sqrt{\Delta^2 + \mu_{L,R}^2}$. When the magnetic field B is close to Δ , one can change the signs of $g_{L,R}$ by changing $\mu_{L,R}$ respectively.

2.3 Hight and low modes

Though the wavefunctions of (2.2) can be found explicitly, their form is enough complicated to stall any further analysis. However, as the spin-orbit energy is assumed to be the biggest energy scale for a homogeneous wire, one can reduce the Hamiltonian (2.2) to:

$$H = \left(\frac{p^2}{2m} + up\sigma_z \right) \tau_z \quad (2.8)$$

in this problem it's reasonably to assume the low energy limit, as all the Majorana physics should live at the energies of the order of g . Thus the energy term must be omitted in Schroedinger equation, which leads to two types of momenta: $p_{short} \approx \pm 2mu$ and $p_{long} \approx 0$ and, respectively two types of wavefunctions: shortwave and longwave ones. The fact that p_{long} is equal to zero means, that the approximation (2.8) is insufficient to describe them. However, to deal with long-wave wavefunctions one can omit the quadratic term in (2.2) and work with linearized Hamiltonian, similar to the ones used in [1] and [2].

Chapter 3

Stationary properties

3.1 Boundary conditions

To obtain the spectrum of the system it's necessary to find the boundary conditions. As the barrier chemical potential is the biggest energy parameter of the problem, the wave-functions there are defined by the Hamiltonian:

$$H(y) = \left(\frac{p^2}{2m} + \mu_b \right) \tau_z, \quad -\frac{L}{2} < y < \frac{L}{2} \quad (3.1)$$

as the low energies are the under consideration, in Sroedinger equation the energy term can be omitted, so $p_b \approx \pm i\sqrt{2m\mu_b}$. One can solve the problem given by (3.1) and match the values of the wavefunction and it's derivatives on the left and on the right of the barrier to obtain:

$$\begin{cases} \psi_L + b\partial_y\psi_L = t(\psi_R + b\partial_y\psi_R) \\ \psi_R - b\partial_y\psi_R = t(\psi_L - b\partial_y\psi_L) \end{cases} \quad (3.2)$$

here $\psi_{L,R} = \psi(\mp \frac{L}{2})$, $b = (2m\mu_b)^{-\frac{1}{2}}$ — the penetration depth for the particle inside th barrier and $t = e^{-\frac{L}{b}}$ — the tunneling constant assumed to be small: $t \ll 1$. This condition reads, that the size of the barrier L should be much bigger that the penetration depth b .

This condition is invariant under the combined action $L \leftrightarrow R, y \rightarrow -y$. To simplify the further analysis one can reverce th direction in the left wire and put both ands of the wires from $y = \frac{L}{2}$ to $y = 0$. The boundary condition than becomes:

$$\begin{cases} \psi_L - b\partial_y\psi_L = t(\psi_R + b\partial_y\psi_R) \\ \psi_R - b\partial_y\psi_R = t(\psi_L + b\partial_y\psi_L) \end{cases} \quad (3.3)$$

This transformation is illustrated on the fig 3.1.

The boundary condition (3.3) can be rewritten with introducing the spinor $\Psi = (\psi_L, \psi_R)^T$

and Pauli matrices s_i in LR space:

$$(1 - ts_x) \Psi - (1 + ts_x) b \partial_y \Psi = 0 \quad (3.4)$$

since for all $t \neq 1$ (recall, that $t \ll 1$) the matrix is $1 \pm ts_x$ in reversible. Multiplying the last equation by $(1 - ts_x) / (1 + t^2)$ one obtain:

$$(1 - 2\tilde{t} - \tilde{b} \partial_y) \psi = 0 \quad (3.5)$$

where $\tilde{t} = \frac{t}{1+t^2}$, $\tilde{b} = \frac{1-t^2}{1+t^2}b$. In the leading order on t , which corresponds to the tunneling limit, $\tilde{t} = t$, $\tilde{b} = b$.

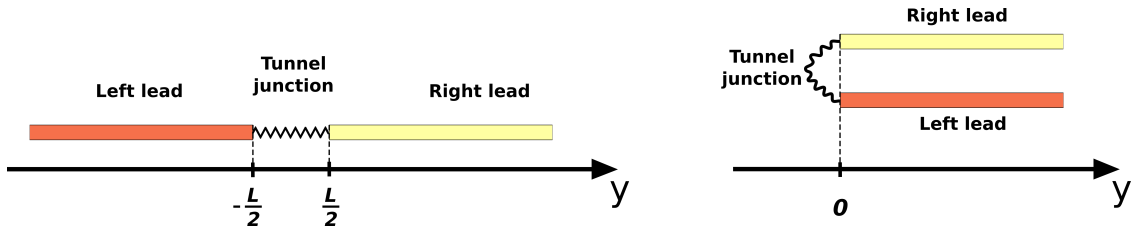


Figure 3.1: Illustration of switching the direction of left wire

One can argue, that in tunneling limit the second and the third term in (3.5) are much smaller than the first one and should not be taken when the leading order is considered. However, if the second terms is omitted, the leads become efficiently disconnected, and no tunnel effects can be found. The same is true for the third term — if it's not present, the boundary condition immediately implies $\Psi(0) = 0$, so the wires become disconnected again.

3.2 High momentum modes

As was pointed in section 2.3, there are two shortwave and longwave wavefunctions inside the wire, and the first ones can be described with the Hamiltonian (2.8). However, if one is looking for the localized states, even the longwave modes should be taken decaying. To obtain this, one needs to add a restore superconducting term in (2.8), so the spectrum become gapped and the momenta can get an imaginary part. So, for shortwave modes one should consider a Hamiltonian:

$$H = \left(\frac{p^2}{2m} - ups_z \sigma_z \right) \tau_z + \Delta \tau_\phi \quad (3.6)$$

here the multiplier s_z is added in the spin-orbit coupling term, as the direction of the left wire is inverted, so to write a correct Hamiltonian for LR space, one needs to change p to $-p$ for the left wire — which is exactly adding $-s_z$ multiplier to each momentum.

Denoting $\eta = \frac{p^2}{2m} - up s_z \sigma_z$, one can rewrite (3.6) as $H = \eta \tau_z + \Delta \tau_\phi$. As $s_z \sigma_z$ commutes with H one can treat it as a number, so the dispersion is $E^2 = \eta^2 + \Delta^2$. Thus $\eta = \pm i \sqrt{\Delta^2 - E^2}$, as the case $|E| < \Delta$ is assumed. For shortwave one can write the equation:

$$p^2 - 2mus_z \sigma_z p - 2m\eta = 0 \quad (3.7)$$

which for shortwave momenta gives $p_{short} \approx 2mus_z \sigma_z + \frac{\eta}{u} s_z \sigma_z$. Choosing the sign of η in a way, that the wavefunction decays at $x \rightarrow \infty$, one can obtain:

$$p_{short} \approx 2mus_z \sigma_z + i \frac{\sqrt{\Delta^2 - E^2}}{u} \quad (3.8)$$

Now the wavefunction can be constructed by putting (3.8) into the Schroedinger equation $(\eta \tau_z + \Delta \tau_\phi) \Psi = E \Psi$. The solutions are:

$$\Psi_{s_z, \sigma_z}(x) = \begin{pmatrix} 1 \\ e^{i(s_z \sigma_z \gamma + \phi_{s_z})} \end{pmatrix}_{eh} e^{2imus_z \sigma_z x - \frac{\sqrt{\Delta^2 - E^2}}{u} x} |s_z, \sigma_z\rangle \quad (3.9)$$

where s_z and σ_z should be treated as numbers can be equal ± 1 , $|s_z, \sigma_z\rangle$ are eigenvectors of matrix $s_z \sigma_z$ and $\gamma = -\frac{\pi}{2} + \arcsin \frac{E}{\Delta}$. Thus the longwave part of eqigenstate can be written as:

$$\Psi_{long} = \sum_{s_z=\pm 1} \sum_{\sigma_z=\pm 1} \Psi_{s_z, \sigma_z}(x) \quad (3.10)$$

and

Bibliography

- ¹Y. Oreg, G. Refael, and F. von Oppen, “Helical liquids and majorana bound states in quantum wires”, Phys. Rev. Lett. **105** (2010).
- ²R. Lutchyn, J. Sau, and D. Sarma, “Majorana fermions and a topological phase transition in semiconductor-superconductor heterostructures”, Phys. Rev. Lett. **105** (2010).